Editors' Suggestion | Featured in Physics

Using Acoustic Perturbations to Dynamically Tune Shear Thickening in Colloidal Suspensions

Prateek Sehgal,[1,*] Meera Ramaswamy,[2,†] Itai Cohen,[2,‡] and Brian J. Kirby[1,3,§]
[1]Sibley School of Mechanical and Aerospace Engineering, Cornell University, Ithaca, New York 14853, USA
[2]Department of Physics, Cornell University, Ithaca, New York 14853, USA
[3]Department of Medicine, Division of Hematology and Medical Oncology, Weill–Cornell Medicine, New York, New York 10021,USA

(Received 16 May 2019; published 17 September 2019)

Colloidal suspensions in industrial processes often exhibit shear thickening that is difficult to control actively. Here, we use piezoelectric transducers to apply acoustic perturbations to dynamically tune the suspension viscosity in the shear-thickening regime. We attribute the mechanism of dethickening to the disruption of shear-induced force chains via perturbations that are large relative to the particle roughness scale. The ease with which this technique can be adapted to various flow geometries makes it a powerful tool for actively controlling suspension flow properties and investigating system dynamics.

DOI: 10.1103/PhysRevLett.123.128001

The orders-of-magnitude increase in viscosity that arises under high shear makes dense suspensions ideal for numerous industrial applications including shock absorption, damping, soft-body armor, astronaut suits, and curved-surface polishing [1–6]. The challenge in using such shear thickening fluids, however, is that this same increase in viscosity can lead to jamming and failure of pumping and mixing equipment driving the flows. The ability to manage these limitations of this important technological material remains challenging [1,7] because it requires actively tuning the suspension viscosity. Shear thickening viscosity previously has been tuned passively by changing the physical properties of the suspension constituents, such as the volume fraction (ϕ) [8–10], particle size [11], particle shape [12,13], roughness [14,15], surface chemistry [16], and solvent attributes [2,17–19], all of which affect the formation of the force chains responsible for thickening [9,11,16,20–33]. However, active tuning to change the flow properties on demand without changing the physical properties of the suspension constituents or without modifying the suspension has until recently remained largely unexplored.

Recently, it was shown that macroscopic boundary oscillations can be used to actively tune shear thickening in a dense suspension [34]. The dethickening mechanism entails disruption of the force chains through application of an oscillatory shear flow orthogonal to the primary flow direction. Further simulations explored the parameter space for active tuning and showed that this mechanism is robust and that such orthogonal mechanical perturbations can tune the suspension viscosity over a wide range of shear rates and volume fractions [35]. Unfortunately, using macroscopic boundary oscillations to introduce orthogonal perturbations is not practical for many applications.

Here, we determine whether externally applied acoustic perturbations can be used to actively tune the suspension viscosity in the shear thickening regime. The advantage of this approach is that acoustic perturbations can controllably manipulate particles [36–43] and can be applied via readily available piezoelectric transducers that are bonded to otherwise fixed surfaces [40,44,45]. The key principle motivating our work is that nanoscale acoustic disturbances will locally perturb particles and break the force chains

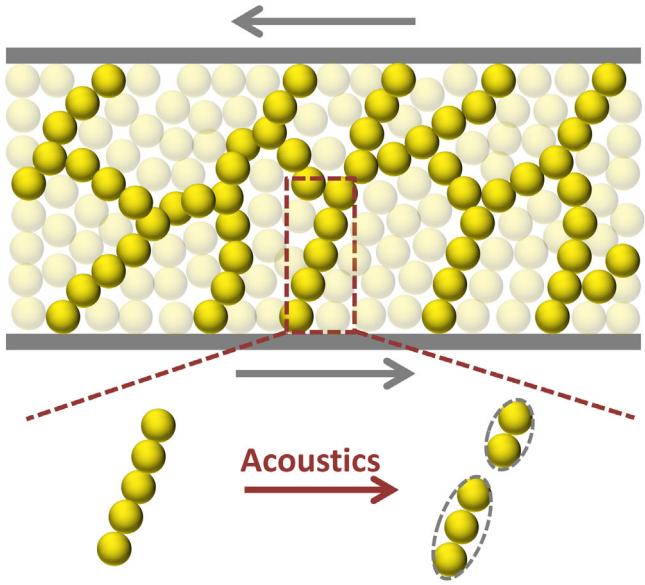

FIG. 1. Hypothesized mechanism of dethickening. (Top) A schematic of the force chain network that forms in dense colloidal suspensions under shear. Gray arrows indicate the shear direction. (Bottom) Spatially nonuniform displacements of the particles in an acoustic field break the fragile force chains, and reduce the viscosity.

responsible for thickening (Fig. 1). From previous studies [13,14,18,34,46], we hypothesize that, to break force chains and achieve dethickening, such perturbations should generate relative particle displacements greater than the particle surface roughness scale and on timescales faster than the turnover rate for the force chains. In our system, the acoustic perturbations can generate nonuniform particle displacements [47] over the length of the force chains, and because these force chains are fragile [20,21], there can be a weak link in the chain where two particles are displaced beyond the surface roughness, resulting in breaking of the chain. In addition, in dense suspensions where interparticle distance is small, the particle contacts may further be disrupted by the acoustic scattering effects from nearby particles [48] and bulk flows due to acoustic dissipation [49]. Furthermore, a typical ultrasonic transducer can apply these acoustic perturbations at timescales that are orders of magnitude shorter than the force chain turnover time, which is typically $\sim 1/\dot{\gamma}$ and $O(\sim 1\ \mathrm{s})$ in our system, where $\dot{\gamma}$ is the strain rate. Thus, we anticipate that acoustic perturbations can disrupt the force chains in a thickened suspension and actively tune the viscosity.

We test this idea on a dense silica colloidal suspension undergoing controlled shear and simultaneous acoustic excitation. Our suspension consists of charge-stabilized silica particles, 2 μm in diameter, in dipropylene glycol at volume fractions of $\phi = 0.53$ and $\phi = 0.50$. Using atomic force microscopy, we measured the average particle surface roughness to be ~ 2 nm, which is well below the estimated dipolar oscillation amplitude (Fig. 2). Our testing apparatus consists of a piezoelectric disk (APC International, Material 841) of diameter 21 and thickness 1.80 mm bonded via epoxy to an aluminum (6061-T6) bottom plate of diameter 19 and thickness 8.57 mm [Fig. 3(a)]. The acoustic perturbations are generated by exciting the piezoelectric crystal in the thickness mode at a resonance frequency $f_r = 1.15$ MHz. This mode applies perturbations in the gradient direction of the primary shear flow. The bottom plate thickness is optimized for maximum energy transfer to the suspension. The piezo-plate setup is integrated with an Anton-Paar MCR702 Rheometer, and a glass top plate is used to apply the primary shear flow and measure the shear viscosity. The suspension is confined between the two plates and the gap is set to 0.64 mm (see the Supplemental Material, Sec. I for calibration [50]). Using this setup, we quantify the effects that acoustic perturbations have on the shear-thickening behavior of our suspensions.

In our measurement protocol, we apply a steady shear to thicken the suspension. After the suspension reaches steady state, we add an amplitude-modulated (AM) acoustic perturbation. The voltage signal used to drive the piezoelectric element has the form $V = V_0[1 + \sin(2\pi f_m t + \Phi_0)]\sin(2\pi f_r t)$, where f_r is the resonance frequency, and $f_m = 0.2$ Hz is the modulation frequency (Fig. S2 [50]). The phase Φ_0 is set arbitrarily

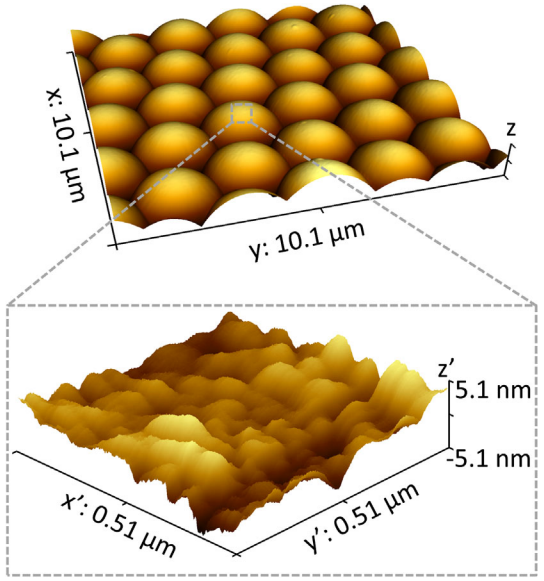

FIG. 2. Surface roughness of the particles measured by atomic force microscopy. (Top) A scan of 10.1 μm × 10.1 μm area of the particle crystal. (Bottom) A scan of 0.51 μm × 0.51 μm area over a single particle surface. The spherical form of the particle is subtracted to obtain the roughness profile in the bottom image (see the Supplemental Material, Sec. II for details on AFM measurements [50]).

and the voltage V_0 is set at 2.5 V to obtain maximum peak-to-peak voltage (V_{pp}) of 10 V. This approach quantifies the dynamic, phase-sensitive, and power-dependent viscosity response of the suspension in a single measurement. The dynamic response probes the important timescales that govern the formation and breakup of force chain. The phase-sensitive response obtained from the controlled modulation eliminates noise in the temporal measurements of the viscosity. Finally, the power-dependent response quantifies the efficiency of this dethickening method. We perform these measurements for a range of strain rates ($\dot{\gamma}$) over which the fluid behavior varies from a Newtonian to a fully thickened state.

As hypothesized, the viscosity response of the thickened suspension depends sensitively on the acoustic perturbations [Fig. 3(b) and Fig. S4 [50]]. For $\phi = 0.53$ suspension sheared at strain rates corresponding to the thickened regime ($\dot{\gamma} = 0.703\ \mathrm{s}^{-1}$), the instantaneous relative viscosity, η_r, oscillates when the acoustic perturbations are applied. The oscillations result from the amplitude modulation of the acoustic perturbations with the greatest decrease in viscosity arising from the largest perturbation amplitude. The minima of these viscosity oscillations are still above the Newtonian viscosity, which suggests that a higher acoustic power is required to break up all the force chains. In contrast, for strain rates corresponding to the unthickened Newtonian regime ($\dot{\gamma} = 0.111\ \mathrm{s}^{-1}$) we observe no modulations in the viscosity. This difference

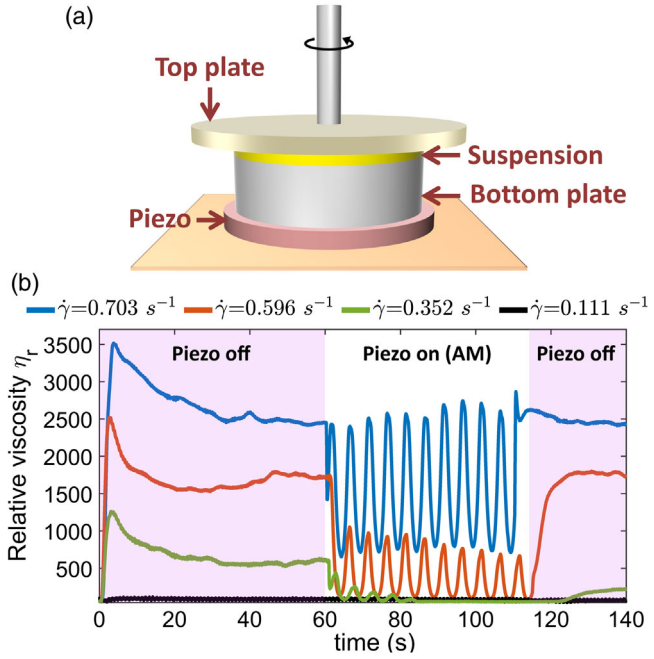

FIG. 3. Experimental setup and AM measurements. (a) The schematic of the acoustic-rheometer setup. The top plate is connected to the rheometer and the bottom plate is bonded to the piezoelectric element. The suspension is confined between the two plates. (b) The instantaneous viscosity response of $\phi = 0.53$ suspension to the gradient-direction perturbations at representative strain rates. The relative viscosity is defined as the ratio of the suspension viscosity to the solvent (dipropylene glycol, 0.11 Pa s) viscosity. Each measurement is performed at a steady $\dot{\gamma}$ for 140 s in which the AM signal is turned on at time $t \sim 60$ s for at least nine modulation cycles, followed by an off-period for the remaining time. Measurements for $\phi = 0.50$ suspension are shown in Supplemental Material, Fig. S4 [50].

in response is consistent with the proposed mechanism that the acoustic perturbations break the shear induced force chains responsible for thickening, leaving the other suspension properties largely unchanged.

For strain rates corresponding to the transition regime between the Newtonian and fully thickened state ($\dot{\gamma} = 0.596,\ 0.352\ \mathrm{s}^{-1}$), the acoustic perturbations are sufficient to dethicken the suspension viscosity to the value in the Newtonian regime. Interestingly, the maximum viscosity during the time when AM perturbations are applied does not recover fully to the steady state value. We interpret this response to indicate that the AM frequency is too rapid for the force chains to fully form between successive oscillations at these strain rates. This picture is supported by the fact that the viscosity recovery time when the perturbations are turned off is much longer than the AM oscillation period.

We extract the magnitude of acoustic dethickening as a function of strain rates using a phase-sensitive analysis of the instantaneous viscosity response curves (Fig. 4, see Supplemental Material, Sec. IV for details [50]). We observe that the application of the acoustic perturbations decreases the viscosity substantially in the regime where the suspension thickens. This response is sensitive to the strain rate, with the largest decrease occurring in the transition regime [Figs. 4(a) and 4(b)]. We quantify this response by plotting the %Reduction in viscosity vs $\tilde{\dot{\gamma}}$, the strain rate normalized by the strain rate at the onset of thickening [Fig. 4(c)]. We find a negligible decrease in the viscosity in the Newtonian regime ($\tilde{\dot{\gamma}} < 1$), in which the force chains are mostly absent. We find the highest reduction in the transition region ($1 < \tilde{\dot{\gamma}} < 2$), in which the applied acoustic perturbations are sufficient to break up the majority of the force chains. This decrease in viscosity to nearly the Newtonian value effectively shifts the onset strain rate for thickening. Finally, we find that the %Reduction decreases and plateaus in the fully thickened regime ($2 < \tilde{\dot{\gamma}}$). This plateau is consistent with literature predictions that the force chain network saturates in the thickened regime [9] and with the idea that the acoustic perturbations are only breaking up a fraction of this

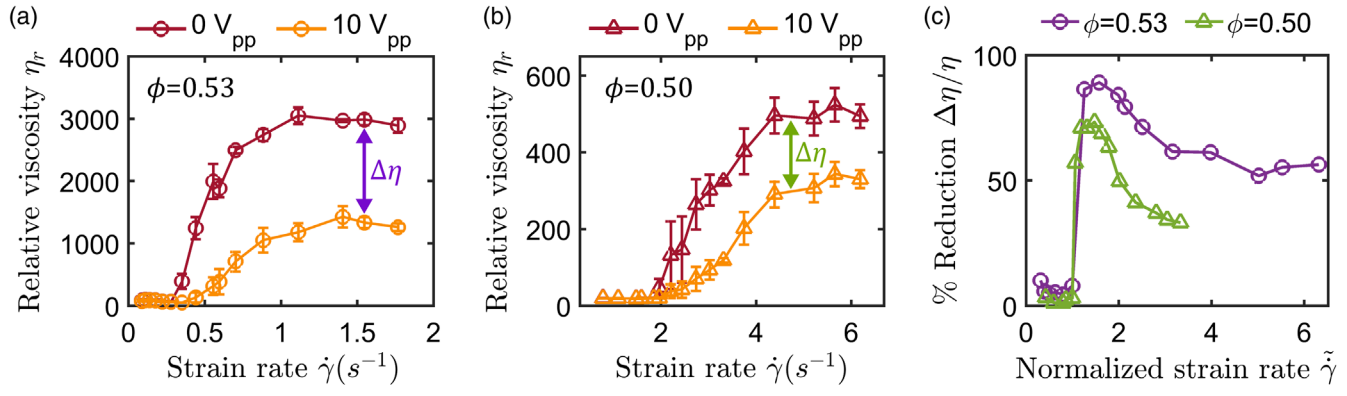

FIG. 4. Dethickening response to the acoustic perturbations for (a) $\phi = 0.53$ and (b) $\phi = 0.50$ suspensions. Relative viscosity η_r vs strain rate $\dot{\gamma}$ is plotted for no perturbations (maroon curve) and 10 V_{pp} perturbations (yellow curve). The viscosities are obtained from Fig. 3(b) via a phase sensitive analysis that reduces temporal noise (see Supplemental Material, Sec. IV for details [50]). (c) Percentage reduction in the viscosity at different normalized strain rates $\tilde{\dot{\gamma}}$ upon application of 10 V_{pp} signal in $\phi = 0.53$ and $\phi = 0.50$ suspensions.

network at this power. The trends at each volume fraction are similar, but dethickening is lower in $\phi = 0.50$ suspensions than in $\phi = 0.53$ suspensions. This difference in effect magnitude is consistent with the results from boundary oscillation simulations [35]. Collectively, these data suggest that a further increase in power would shift the onset of the thickening to higher strain rates or stress scales [30], and increase the dethickening in the thickened regime.

Using the AM protocol, we determine the power-dependent response of the suspension and observe a logarithmic decrease in the viscosity above a threshold power (Fig. 5). We define a normalized viscosity $\bar{\eta} = (\eta - \eta_{\min})/(\eta_{\max} - \eta_{\min})$, where $\eta_{\max}$ and $\eta_{\min}$ are the maximum and minimum viscosities at given $\dot{\gamma}$ during a modulation period. We plot $\bar{\eta}$ vs power for strain rates in which the turnover time of force chains is substantially faster than the time period of the AM signal [e.g., blue curve in Fig. 3(b)]. Strikingly, we find a thresholdlike behavior at very low powers (inset Fig. 5), where the viscosity decrease is very slow and negligible up to powers ~5 mW (corresponding to $V_{pp} = 1.4$ V). This trend is consistent with our mechanistic hypothesis that a minimum particle displacement is required to break force chains. Beyond this threshold, the viscosity initially decreases rapidly at lower powers up to ~0.08 W (orange curve in Fig. 5), which suggests that a significant number of force chains are broken even at a small input power. At higher power, the viscosity decreases more slowly. This nonlinear evolution suggests that although a higher power is required to completely eliminate the thickening effects of force chains, a large fraction of dethickening can be achieved by just small input power.

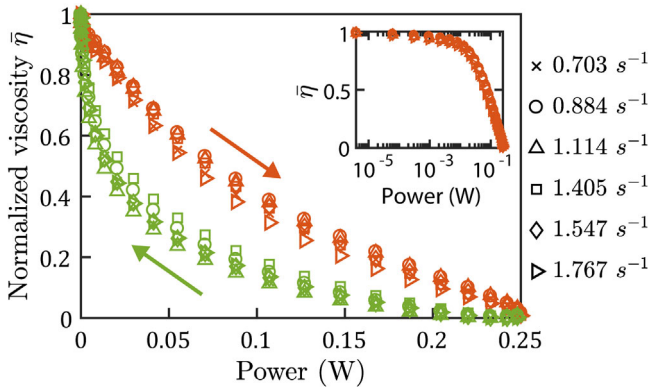

FIG. 5. Evolution of viscosity with input power at different strain rates (markers) for $\phi = 0.53$ suspensions. Normalized viscosity $\bar{\eta}$ is calculated from the Fourier analysis of the data in Fig. 3(b) (See Supplemental Material, Sec. IV [50]). Orange markers show the decrease in viscosity when the power is ramped up and green markers show the subsequent increase in viscosity when the power is ramped down. A power analysis confirms that thermal contributions to the observed dethickening response are negligible (see Supplemental Material, Sec. VI [50]). (Inset) Evolution of normalized viscosity with the ramp up of power (orange markers) on a semi-log plot. Power-dependent response for $\phi = 0.50$ suspensions is shown in Supplemental Material, Fig. S5 [50].

As the power is ramped down (green curve), we observe a hysteretic response indicating that while a larger power is needed to break up the force chains, a significantly lower power is needed to maintain this disruption during this period. These results suggest that the suspension retains some memory of the microstructure within each AM cycle even though the modulation time period is large enough for the force chains to fully recover. Our findings are consistent with the simulations of orthogonal boundary oscillations that indicate a dethickened viscosity can be maintained using pulsed perturbations [35]. Our ability to precisely measure these hysteresis loops shows that this amplitude modulation technique can determine the relevant timescales to form and break force chains. This understanding can then be leveraged to optimize strategies for achieving dethickening with minimal amount of power.

For the current implementation of these acoustic modulations, the power required to dethicken the suspension is over an order of magnitude higher than the power required for shearing the thickened suspension. Further studies, aimed at improving the coupling of acoustic energy to the suspension and applying perturbation intermittently, may change this balance. Moreover, the particle displacements that are driving these changes in the viscosity maybe complex in the dense suspensions because of the acoustic scattering from nearby particles, bulk acoustic flows, and steric constraints. Measurements or simulations of the exact particle displacements are required to confirm their hypothesized mechanistic link with the particle roughness. This understanding of the suspension microstructure upon acoustic excitation and development of strategies for enhancing disruptions should also enable more efficient control of the suspension viscosity.

Even in its current form, however, our method has paramount advantages in the applications where the goal is to increase the flow rate, unclog a system, or control the viscosity, without energy concerns. Such applications include high-throughput processing of dense suspensions, avoiding jamming in narrow conduits, 3D printing, and designing of smart materials. In each of these cases, the perturbations can be applied by simply bonding a piezoelectric element to a fixed surface, which makes this method easy to integrate with the existing practical systems without modifying their geometry. Furthermore, acoustic perturbations can tune thickening in these applications in multiple modes, thus providing flexibility in implementation (see Supplemental Material, Sec. VII [50] for data on acoustic perturbations in the vorticity direction). Overall, our method has laid a strong foundation to robustly design smart transport systems that handle shear-thickening fluids.

We thank Anton Paar for use of the MCR 702 rheometer through their VIP academic research program, Abhishek Shetty for help with the rheometer, the Kirby group and the

Cohen group for their insightful suggestions, Professor Wolfgang Sachse at Cornell for lending equipment and useful discussions, and the Amit Lal group at Cornell for providing the impedance analyzer. This work is supported by NSF CBET Grants No. 1804963, No. 1232666, and No. 1509308, partially supported by the Center on the Physics of Cancer Metabolism through Grant No. 1U54CA210184-01, and performed in part at the Cornell NanoScale Facility, an NNCI member supported by NSF Grant No. NNCI-1542081.

P. S. and M. R. contributed equally to this work.

*ps824@cornell.edu
†mr944@cornell.edu
‡itai.cohen@cornell.edu
§kirby@cornell.edu

[1] E. Brown and H. M. Jaeger, Rep. Prog. Phys. **77**, 046602 (2014).
[2] N. J. Wagner and J. F. Brady, Phys. Today **62**, No. 10, 27 (2009).
[3] C. Fischer, S. A. Braun, P.-E. Bourban, V. Michaud, C. J. G. Plummer, and J.-A. E. Månson, Smart Mater. Struct. **15**, 1467 (2006).
[4] Y. S. Lee, E. D. Wetzel, and N. J. Wagner, J. Mater. Sci. **38**, 2825 (2003).
[5] M. Li, B. Lyu, J. Yuan, C. Dong, and W. Dai, Int. J. Mach. Tools Manuf. **94**, 88 (2015).
[6] C. D. Cwalina, C. M. McCutcheon, R. D. Dombrowski, and N. J. Wagner, Compos. Sci. Technol. **131**, 61 (2016).
[7] H. A. Barnes, J. Rheol. **33**, 329 (1989).
[8] C. D. Cwalina and N. J. Wagner, J. Rheol. **60**, 47 (2016).
[9] R. Mari, R. Seto, J. F. Morris, and M. M. Denn, J. Rheol. **58**, 1693 (2014).
[10] M. M. Denn, J. F. Morris, and D. Bonn, Soft Matter **14**, 170 (2018).
[11] B. M. Guy, M. Hermes, and W. C. K. Poon, Phys. Rev. Lett. **115**, 088304 (2015).
[12] C. D. Cwalina, K. J. Harrison, and N. J. Wagner, AIChE J. **63**, 1091 (2017).
[13] L. C. Hsiao, S. Jamali, E. Glynos, P. F. Green, R. G. Larson, and M. J. Solomon, Phys. Rev. Lett. **119**, 158001 (2017).
[14] C.-P. Hsu, S. N. Ramakrishna, M. Zanini, N. D. Spencer, and L. Isa, Proc. Natl. Acad. Sci. U.S.A. **115**, 5117 (2018).
[15] D. Lootens, H. van Damme, Y. Hémar, and P. Hébraud, Phys. Rev. Lett. **95**, 268302 (2005).
[16] W. Yang, Y. Wu, X. Pei, F. Zhou, and Q. Xue, Langmuir **33**, 1037 (2017).
[17] E. Brown, N. A. Forman, C. S. Orellana, H. Zhang, B. W. Maynor, D. E. Betts, J. M. DeSimone, and H. M. Jaeger, Nat. Mater. **9**, 220 (2010).
[18] N. M. James, E. Han, R. A. L. de la Cruz, J. Jureller, and H. M. Jaeger, Nat. Mater. **17**, 965 (2018).
[19] B. J. Maranzano and N. J. Wagner, J. Rheol. **45**, 1205 (2001).
[20] M. E. Cates, J. P. Wittmer, J.-P. Bouchaud, and P. Claudin, Phys. Rev. Lett. **81**, 1841 (1998).
[21] T. S. Majmudar and R. P. Behringer, Nature (London) **435**, 1079 (2005).
[22] R. Seto, R. Mari, J. F. Morris, and M. M. Denn, Phys. Rev. Lett. **111**, 218301 (2013).
[23] J. F. Morris, Phys. Rev. Fluids **3**, 110508 (2018).
[24] D. Bi, J. Zhang, B. Chakraborty, and R. P. Behringer, Nature (London) **480**, 355 (2011).
[25] J. Comtet, G. Chatté, A. Niguès, L. Bocquet, A. Siria, and A. Colin, Nat. Commun. **8**, 15633 (2017).
[26] C. Clavaud, A. Bérut, B. Metzger, and Y. Forterre, Proc. Natl. Acad. Sci. U.S.A. **114**, 5147 (2017).
[27] N. Y. C. Lin, B. M. Guy, M. Hermes, C. Ness, J. Sun, W. C. K. Poon, and I. Cohen, Phys. Rev. Lett. **115**, 228304 (2015).
[28] J. R. Royer, D. L. Blair, and S. D. Hudson, Phys. Rev. Lett. **116**, 188301 (2016).
[29] N. Fernandez, R. Mani, D. Rinaldi, D. Kadau, M. Mosquet, H. Lombois-Burger, J. Cayer-Barrioz, H. J. Herrmann, N. D. Spencer, and L. Isa, Phys. Rev. Lett. **111**, 108301 (2013).
[30] M. Wyart and M. E. Cates, Phys. Rev. Lett. **112**, 098302 (2014).
[31] E. Brown and H. M. Jaeger, J. Rheol. **56**, 875 (2012).
[32] J. E. Thomas, K. Ramola, A. Singh, R. Mari, J. F. Morris, and B. Chakraborty, Phys. Rev. Lett. **121**, 128002 (2018).
[33] V. Rathee, D. L. Blair, and J. S. Urbach, Proc. Natl. Acad. Sci. U.S.A. **114**, 8740 (2017).
[34] N. Y. C. Lin, C. Ness, M. E. Cates, J. Sun, and I. Cohen, Proc. Natl. Acad. Sci. U.S.A. **113**, 10774 (2016).
[35] C. Ness, R. Mari, and M. E. Cates, Sci. Adv. **4**, eaar3296 (2018).
[36] D. J. Collins, R. O'Rorke, C. Devendran, Z. Ma, J. Han, A. Neild, and Y. Ai, Phys. Rev. Lett. **120**, 074502 (2018).
[37] P. Sehgal and B. J. Kirby, Anal. Chem. **89**, 12192 (2017).
[38] S. M. Naseer, A. Manbachi, M. Samandari, P. Walch, Y. Gao, Y. S. Zhang, F. Davoudi, W. Wang, K. Abrinia, J. M. Cooper, A. Khademhosseini, and S. R. Shin, Biofabrication **9**, 015020 (2017).
[39] M. X. Lim, A. Souslov, V. Vitelli, and H. M. Jaeger, Nat. Phys. **15**, 460 (2019).
[40] M. Antfolk, P. B. Muller, P. Augustsson, H. Bruus, and T. Laurell, Lab Chip **14**, 2791 (2014).
[41] G. Destgeer, A. Hashmi, J. Park, H. Ahmed, M. Afzal, and H. J. Sung, RSC Adv. **9**, 7916 (2019).
[42] P. B. Muller, M. Rossi, A. G. Marín, R. Barnkob, P. Augustsson, T. Laurell, C. J. Kähler, and H. Bruus, Phys. Rev. E **88**, 023006 (2013).
[43] X. Ding, S.-C. S. Lin, B. Kiraly, H. Yue, S. Li, I.-K. Chiang, J. Shi, S. J. Benkovic, and T. J. Huang, Proc. Natl. Acad. Sci. U.S.A. **109**, 11105 (2012).
[44] T. Laurell, F. Petersson, and A. Nilsson, Chem. Soc. Rev. **36**, 492 (2007).
[45] A. Lenshof, M. Evander, T. Laurell, and J. Nilsson, Lab Chip **12**, 684 (2012).
[46] M. M. Denn and J. F. Morris, Annu. Rev. Chem. Biomol. Eng. **5**, 203 (2014).
[47] H. Bruus, Lab Chip **12**, 1014 (2012).
[48] G. T. Silva and H. Bruus, Phys. Rev. E **90**, 063007 (2014).
[49] M. Wiklund, R. Green, and M. Ohlin, Lab Chip **12**, 2438 (2012).
[50] See Supplemental Material at http://link.aps.org/supplemental/10.1103/PhysRevLett.123.128001 for details of the setup and equipment used, additional data and analysis, and results from the vorticity direction perturbations.